Title

Dipolar Assisted Assignment Protocol (DAAP) for MAS solid-state NMR of rotationally aligned membrane proteins in phospholipid bilayers

Authors

Das, Bibhuti B
Zhang, Hua
Opella, Stanley J

Publication Date

2014-05-01

DOI

10.1016/j.jmr.2014.02.018

Peer reviewed

Published in final edited form as:
J Magn Reson. 2014 May ; 242: 224–232. doi:10.1016/j.jmr.2014.02.018.

Dipolar Assisted Assignment Protocol (DAAP) for MAS solid-state NMR of Rotationally Aligned Membrane Proteins in Phospholipid Bilayers

Bibhuti B. Das, **Hua Zhang**, and **Stanley J. Opella***
Department of Chemistry and Biochemistry, University of California, San Diego, La Jolla, California 92093-0307

Abstract

A method for making resonance assignments in magic angle spinning solid-state NMR spectra of membrane proteins that utilizes the range of hetero-nuclear dipolar coupling frequencies in combination with conventional chemical shift based assignment methods is demonstrated. The dipolar assisted assignment protocol (DAAP) takes advantage of the rotational alignment of the membrane proteins in liquid crystalline phospholipid bilayers. Improved resolution is obtained by combining the magnetically inequivalent heteronuclear dipolar frequencies with isotropic chemical shift frequencies. Spectra with both dipolar and chemical shift frequency axes assist with resonance assignments. DAAP can be readily extended to three- and four- dimensional experiments and to include both backbone and side chain sites in proteins.

Introduction

The resolution and assignment of resonances is a requisite first step in protein structure determination by NMR spectroscopy. The resolution of individual resonances is generally accomplished with multidimensional NMR experiments that correlate chemical shift frequencies among directly bonded and proximate homo- and hetero- nuclei. Protocols for chemical shift-based resonance assignments are now well established for magic angle spinning (MAS) solid-state NMR [1–4]. However, in spite of recent advances in methods, it remains difficult to apply chemical shift-based assignment schemes to membrane proteins in phospholipid bilayers, whether in stationary aligned samples in oriented sample (OS) solid-state NMR [5] or in unoriented samples in MAS solid-state NMR [6]. This is largely because these proteins contain many similar hydrophobic residues in uniform helices whose signals have the same or very similar chemical shifts. Here we describe how the highly variable heteronuclear dipolar couplings observed in rotationally aligned (RA) solid-state NMR spectra of membrane proteins [7] can be used to assist in the resolution and

*Corresponding author: sopella@ucsd.edu.

assignment process by enabling one of the frequency dimensions in multidimensional spectra to be heteronuclear dipolar coupling frequencies rather than chemical shift frequencies. This is an alternative to isotope labeling based schemes that depend on the preparation of multiple samples [8].

Phospholipids and membrane proteins undergo global motions, in particular rapid rotational diffusion about the bilayer normal [9, 10] and translational diffusion in the plane of the bilayer [11, 12]. The rotational motion results in 'rotational alignment' of the proteins that yields frequencies equivalent to those obtained from mechanical or magnetic alignment [10, 13]. This was first demonstrated using ^{31}P NMR of phospholipids by McLaughlin et al [14]. It was shown that a single-line chemical shift frequency observed from a uniaxially oriented bilayer sample and the parallel edge of a rotationally averaged powder pattern from an unoriented bilayer sample are equivalent. Later ^{15}N NMR of single site ^{15}N labeled polypeptide in lipid bilayer [15] also showed this to be the case for membrane proteins in addition to the phospholipids. An early experiment by Griffin and colleagues demonstrated that ^{13}C′-labeled bacteriorhodopsin in unoriented phospholipid bilayers undergoes rotational diffusion around the bilayer normal and importantly that the motion can be switched on and off reversibly by varying the sample temperature [16]. The global motion is either frozen completely or slow enough at lower temperature (below the gel to liquid crystalline phase transition temperature of the phospholipids) to enable the static powder pattern to be observed. Similar results have been obtained for several expressed proteins [15, 17] including a seven transmembrane helix G-protein coupled receptor [2, 18, 19]. This enabled the measurement of orientationally-dependent frequencies werfrom unoriented samples of membrane proteins labeled with ^{15}N and ^{13}C nuclei [7, 19].

The global rotation of the protein occurs fast enough ($\tau_c \sim 10^{-6}$ s) to motionally average one-bond ^{1}H-^{13}C and ^{1}H-^{15}N heteronuclear dipolar coupling (DC) powder patterns in a predictable way. They are axially symmetric, and the span of the powder pattern is reduced by an amount that depends upon the angle between the bond axis and the direction of rotation, in this case the bilayer normal. This defines rotational alignment, a fundamental principle of solid-state NMR demonstrated in some of the earliest experiments for homonuclear dipolar couplings and chemical shift anisotropy [20, 21]. Of direct relevance for structural studies of membrane proteins, the alignment resulting from the rotational motion of the protein about the bilayer normal makes it possible to measure the equivalent angular constraints from unoriented proteoliposome sample as from stationary uniaxially aligned samples [19]. Importantly, in both cases, angles are measured relative to a single external axis (the bilayer normal in the case of RA solid-state NMR), which means that errors do not accumulate. The resulting angular constraints are a major source of input for the calculation of protein structures [7].

Experiments for dipolar assisted resolution and assignment of protein resonances are described in this article. The resolution and assignment method starts with conventional chemical shift based assignments with the addition of recoupling of hetero-nuclear dipolar frequencies in an additional frequency dimension. We show that much higher overall resolution is achievable from the combination of isotropic chemical shift frequencies and anisotropic heteronuclear dipolar coupling frequencies in rotationally aligned membrane

proteins. Unambiguous resonance assignments are feasible with this approach for residues that are chemically equivalent but have different heteronuclear dipolar couplings due to their orientation relative to the bilayer normal. The method is demonstrated using an expressed 36-residue polypeptide that includes the residues corresponding to the single helix from the trans-membrane domain of the membrane protein Vpu from HIV-1 (Vpu TM). Even though this polypeptide is relatively small, it provides a rigorous test of the method because it has so many similar hydrophobic residues in its highly regular trans-membrane helix. It was difficult to assign using conventional approaches. Overall, the methods are highly effective in structural studies because in addition to spectral resolution and resonance assignments, structural constraints can be measured from the same three-dimensional spectra.

Methods

Sample preparation

The expression and purification of Vpu TM were performed as previously described [22]. The pET31b(+) vector containing the sequence of Vpu TM fused to that of keto steroid isomerase (KSI) was expressed in C43(DE3) competent cells in isotopically enriched M9 medium suitable for $^{13}C/^{15}N$ double labeling of proteins. Cells were harvested 5 hrs after Isopropyl β-D-1-thiogalactopyranoside induction, lysed by sonication, and then centrifuged to isolate the inclusion bodies containing the Vpu TM fusion protein. Purification was performed by nickel chelating affinity chromatography followed by cyanogen bromide cleavage to separate the Vpu TM target protein from the KSI fusion partner. Lyophilized protein powder was dissolved in 1:4 (v/v) hexafluoro-isopropanol: dichloromethane and sonicated to precipitate the KSI. The organic solution was filtered through a 0.2um PTFE filter and dried to a film with nitrogen gas. Final pure protein powder was obtained by another filtration of the sample in 1:0.998:0.002(v/v) water: hexafluoro-isopropanol: trifluoroacetic acid followed by solvent removal by lyophilization.

To prepare the proteoliposomes samples used in the solid-state NMR experiments, 2 mg of $^{13}C/^{15}N$ labeled Vpu TM and 10mg 1,2-dimyristoyl-sn-glycero-3-phosphocholine (DMPC) were dissolved in 1 ml of 0.5% sodium dodecyl sulfate (SDS) buffer. The mixture was shaken for 2 hr., dialyzed against water for 24 hr., and then dialyzed against a solution containing 20 mM potassium chloride (KCl) for 12 hr. to remove any residual SDS. The sample pH was adjusted to 4.0 followed by ultra-centrifugation at 65,000 rpm for 12 hrs. The pellet was then transferred to a 3.2 mm OD MAS rotor.

The sequence of the polypeptide contains 36 residues; those marked in bold and underlined constitute the trans-membrane helix of Vpu and are analyzed in Table 1 and Figure 8:
QPIQIA**IVA**$_{10}$**LVVAI**$_{15}$**IIAIV**$_{20}$**VWSIV**$_{25}$IIEGRGGKKKK

NMR Spectroscopy

The experimental data were acquired using the pulse sequences diagrammed in Figure 1. In all the experiments, swept frequency two-pulse phase modulation (SW_f-TPPM) [23] with 100 kHz radio frequency (RF) strength was used for ^1H decoupling and 2.5 kHz RF irradiation for ^{15}N decoupling with WALTZ-16 [24] modulation. Cross-polarization (CP)

[25] from ^{1}H to either ^{15}N or ^{13}C was optimized using (50%) amplitude-modulated RF irradiation on the ^{1}H frequency channel. Subsequently, 30 kHz and 60 kHz RF pulses were applied on the ^{15}N and ^{13}C frequency channels, respectively. Varying the CP contact times between 0.1 and 1.0 ms, the carrier frequency offsets, and the decoupling irradiations optimized the sensitivity of individual experiments. Double cross-polarization (DCP) from ^{15}N to ^{13}C was accomplished using spectrally induced filtering in combination with cross-polarization (SPECIFIC-CP) [26]. Adiabatic tangential pulses on the ^{13}C channel were optimized for maximum polarization transfer with RF field strengths of 27 kHz for ^{15}N, 16 kHz for ^{13}C and 38 kHz for ^{13}CO. Magnetization from ^{13}C to ^{15}N was transferred using z-filter transferred-echo double-resonance (z-TEDOR) experiments [27]. In TEDOR-based experiments, 62.5 kHz and 50 kHz RF irradiations were applied on the ^{13}C and ^{15}N frequency channels, respectively. Sixteen rotor periods with XY8 phase cycling were used for recoupling of heteronuclear dipolar couplings. Homonuclear $^{13}C/^{13}C$ correlation in two and three-dimensional experiments was performed using either a 50 ms mixing period under proton driven spin diffusion (PDSD)[28–31] or a 20 ms mixing period with dipolar assisted rotational resonance (DARR) [32].

Recoupling of the hetero-nuclear dipolar coupling frequencies in MAS experiments was performed using symmetry-based $R18^{7}_{1}$ and $R18^{5}_{2}$ pulse schemes [33]. A pair of 180° pulses with a phase modulation of 70° (π_{70}-π_{70}) was employed for the R^{7}_{1} scheme. The scaling factors for the pulse sequences were measured experimentally with ^{13}C and ^{15}N detection using a uniformly ^{13}C, ^{15}N labeled N-acetyl leucine powder sample. The measured dipolar splittings of 6.7 kHz for ^{1}H-^{13}C and 3.4 kHz for ^{1}H-^{15}N correspond to a scaling factor of 0.16. Two- and three-dimensional separated local field (SLF) [34] experiments were performed using direct ^{13}C-detection with ^{15}N filtering. ^{1}H-^{13}C and ^{1}H-^{15}N dipolar coupling frequencies were correlated to the isotropic chemical shift frequencies from ^{13}C and ^{15}N sites.

Three-dimensional SLF experiments correlating ^{1}H-^{15}N DCs with ^{13}C and ^{15}N isotropic chemical shifts were performed using the pulse scheme shown in Figure 1A and B. In Figure 1A, the ^{1}H magnetization was transferred to ^{15}N under Hartmann-Hahn CP followed by the dipolar frequency evolution under $R18^{7}_{1}$ recoupling pulses. The ^{1}H-^{15}N dipolar coupling frequencies are recoupled in a constant time evolution period and are encoded in a third dimension. The ^{15}N magnetization is then flipped back to the laboratory frame using a hard 90° pulse. A z-filter is then employed to dephase remaining magnetization. Low power RF under DARR [32] condition is applied on ^{1}H channel during the z-filter. ^{15}N transverse magnetization is created using a flip back 90° pulse followed by the ^{15}N isotropic chemical shifts evolution encoded in the 2^{nd} dimension. The phase sensitive chemical shifts are recorded in States mode by varying the phase of the flip back 90° pulse. Heteronuclear decoupling during the evolution is achieved with a 180° hard pulse on ^{13}C and SW_{f}-TPPM pulses on ^{1}H. ^{15}N magnetization was then transferred selectively to either ^{13}C or ^{13}CO using DCP followed by the $^{13}C/^{13}C$ spin diffusion mixing period and direct ^{13}C detection under heteronuclear decoupling. Three-dimensional data were acquired correlating ^{1}H-^{15}N DC frequencies with either N(CA)CX or N(CO)CX two-dimensional planes. The pulse scheme provides an opportunity to correlate intra and inter residues in a sequential manner.

In a similar fashion, simultaneous correlation in intra and inter residues is achieved using the pulse scheme shown in Figure 1B. In this projected three-dimensional experiment, the ^{1}H-^{15}N DCs are correlated with ^{15}N, ^{13}C chemical shift frequencies within a residue, and the ^{13}CO shift from the preceding residue. The correlation is established following the steps of coherence transfer pathway. 1.) The ^{1}H magnetization is transferred to ^{13}C using Hartmann-Hahn CP. 2.) Magnetization from ^{13}C is transferred to ^{15}N using TEDOR mixing followed by ^{1}H-^{15}N dipolar coupling frequency evolution under $R18^{7}_{1}$ recoupling pulses. 3.) ^{13}C magnetization is flipped back to the Z-direction followed by a short z-filter period. 4.) ^{15}N transverse magnetization is created using a hard 90° pulse followed by ^{1}H-^{15}N dipolar evolution under recoupling pulses. 5.) Following the dipolar evolution, ^{15}N chemical shifts are encoded under ^{1}H and ^{13}C decoupling. Phase sensitive data are collected by varying the phase of the flip back 90° pulse under States mode followed by the second z-filter. 5.) ^{15}N magnetization is then transferred back to ^{13}C using a second TEDOR mixing followed by a third z-filter. Each of the z-filters is synchronized with two-rotor periods of ^{1}H irradiation under DARR. 6.) In the final step, both ^{13}C and inter residue ^{13}CO signals are acquired directly in the presence of ^{1}H and ^{15}N heteronuclear decoupling.

The measurement of ^{1}H-^{13}C dipolar frequencies within a residue was carried out using the pulse scheme shown in Figure 1C and E. In Figure 1C, the ^{1}H-^{13}C DC is correlated to a two-dimensional ^{13}C/^{13}C homo-nuclear chemical shift correlation. The three-dimensional experiment is carried out following the steps: 1.) ^{13}C magnetization was initially generated by CP from ^{1}H. 2.) ^{1}H-^{13}C dipolar frequencies are recoupled using the symmetry pulse scheme $R18^{7}_{1}$ in a constant time manner. The dipolar frequencies are encoded in a third dimension. 3.) Following the dipolar evolution, phase sensitive isotropic ^{13}C chemical shifts are encoded with hetero-nuclear decoupling. A hard 180° pulse on ^{15}N and SW_f–TPPM pulses for ^{1}H are used for ^{15}N and ^{1}H decoupling. Homonuclear correlation is established using spin diffusion with DAAR or PDSD mixing followed by the direct ^{13}C detection under ^{1}H decoupling.

The pulse sequence diagrammed in Figure 1E correlates ^{1}Hα-^{13}Cα dipolar frequencies with ^{15}N and ^{13}Cα isotropic shifts. This is equivalent to the pulse scheme shown in Figure 1D except that ^{15}N chemical shift is encoded during t1 evolution. ^{15}N shifts are measured in phase sensitive mode by varying the phase of the ^{15}N CP pulse. A 10 s hard pulse for ^{15}N and a 180 s soft pulse with Gaussian shape for ^{13}C nuclei are used for refocusing during the spin echo.

^{1}H-^{15}N and ^{1}Hα-^{13}Cα dipolar frequency correlation within a residue is obtained using the pulse schemes shown in Figure1D. ^{15}N edited ^{13}Cα shifts are correlated with the dipolar frequencies in three-dimensions. The pulse scheme begins with the ^{1}H to ^{15}N CP followed by the ^{1}H-^{15}N dipolar recoupling during t1 evolution. Magnetization is then transferred to ^{13}Cα nuclei using SPECIFIC-CP. ^{1}Hα-^{13}Cα dipolar frequencies are encoded in two orthogonal dimensions following SPECIFIC-CP. Finally; ^{13}Cα signals are detected directly under SW_f-TPPM ^{1}H decoupling.

The experiments were performed on a 750 MHz spectrometer equipped with Bruker Avance console and a 3.2 mm low-E ^{1}H/^{13}C/^{15}N triple-resonance MAS probe. The spinning rate

was controlled at 11.111 kHz ± 2 Hz. Temperature calibration under MAS was carried out using ethylene glycol as an external reference. The ^{1}H chemical shift of water was used to monitor the heating of the protein-containing phospholipid bilayer samples in the presence of strong radiofrequency irradiation. It also served as an internal reference frequency. The chemical shift frequencies were referenced externally to solid samples with the methylene ^{13}C resonance at 38.48 ppm in adamantane and the ammonium sulfate ^{15}N resonance at 26.8 ppm.

Results

Rotational diffusion in phospholipid bilayers

Membrane proteins undergo rotational diffusion about the bilayer normal in liquid crystalline phospholipid bilayers at a rate faster than the NMR interaction timescale ($\tau_c \sim 10^{-6}$ s) [13]. The partial averaging of the powder spectrum depends on the angle between the principal axis of the spin-interaction tensor and the axis of the rotational motion. The most notable effects in the spectra of membrane proteins undergoing fast rotational diffusion are the dramatic reduction in the frequency span of the carbonyl carbon chemical shift powder pattern, and its transformation to axial symmetry [16].

The presence or absence of fast rotational diffusion of Vpu TM reconstituted in DMPC bilayers was monitored as a function of temperature. Here we measure the breadth of the ^{13}CO chemical shift powder using simple one-dimensional ^{13}C detection with 5 kHz “slow” magic angle spinning. As shown in Figure 2A, a family of sidebands is observed at temperatures below ~15 °C; in contrast, essential no side band intensity can be observed above ~25 °C. The sideband intensities are indicative of the breadth and shape of the underlying chemical shift anisotropy powder patterns of the ^{13}CO sites. At low temperatures, the family of side bands represents the rigid lattice powder pattern [35]. On the other hand, the near-total absence of sidebands at higher temperatures confirms that the protein undergoes rotational diffusion. This effect, as plotted in Figure 2B, has also observed in a wide variety of other membrane proteins, including those with seven trans-membrane helices as well as β-barrel membrane proteins.

Resolution in two-dimensional spectra

In order to identify signals associated with the types of amino acid residues in Vpu TM, two-dimensional $^{13}C/^{13}C$ homo-nuclear correlation and $^{15}N/^{13}C$ hetero-nuclear correlation spectra were obtained on a uniformly ^{13}C, ^{15}N labeled sample. The results are shown in Figure 3. These experiments were carried out at 15 °C where the polypeptide is immobile on the relevant NMR timescales (as shown in Figure 2). The $^{13}C/^{13}C$ homo-nuclear correlation spectrum obtained with a 50 ms PDSD mixing time shows high intensity cross-peaks that correlate isotropic chemical shift signals from proximate ^{13}C sites. Resonances from the Ser, Leu, Trp, and Pro residues are labeled in Figure 3A. Dashed lines mark the correlations of ^{13}C resonances in backbone and side chains for the few distinguishable residues in the polypeptide. The overlapped isotropic chemical shifts for the Ala, Val, and Ile residues are also marked; four Ala residues contribute to a single resonance frequency for $^{13}C\alpha$ and $^{13}C\beta$, and only two distinct frequencies in the ^{13}CO region. The highly overlapped

signals from six Val residues show a single frequency for $^{13}C\alpha$, ^{13}CO, as well as side chain sites. The signals from the 10 Ile residues are significantly overlapped with only three distinguishable ^{13}CO resonances, and essentially no resolution among the $^{13}C\alpha$ and side chain carbon frequencies. The two-dimensional $^{15}N/^{13}C$ correlation spectrum in Figure 3B displays somewhat better resolution. Nonetheless, in this two-dimensional N(CA)CX spectrum only ~13 individual signals are distinguishable. Two signals from the Ala and Val residues are well resolved, and ~ 8 signals are recognizable from the 10 Ile residues.

By themselves, three-dimensional experiments correlating resonances from back bone and side chains in a CCC type experiment do little to resolve the severe degeneracies in the chemical shifts of the hydrophobic residues. However, three-dimensional correlation experiments such as NCACX and NCOCX used in sequential assignment show somewhat better resolution [36]. Two-dimensional planes correlating ^{13}C signals from backbone and side chains extracted at ^{15}N shift frequencies are shown in Figure 4. Irrespective of the resolution gain in three-dimensional experiments, unambiguous assignment is not possible due to the overlap of many chemical shift frequencies, for example for V9, V13, I16, I17, I26, I27. However, as shown *infra* the large variation among heteronuclear dipolar coupling frequencies in rotationally aligned samples [7, 19] can be used to increase the resolution and assist in making unambiguous assignments of resonances.

As demonstrated in Figure 2, above 25 °C the protein undergoes rotational diffusion about the bilayer normal resulting in partial averaging of both chemical shift and dipolar coupling powder patterns, which varies depending upon the alignment of the tensors in the molecular frame relative to the bilayer normal. Using symmetry based pulse schemes [33, 37], ^{1}H-^{15}N dipolar frequencies were recoupled and correlated to ^{13}C isotropic chemical shifts in two-dimensional experiments. ^{13}C-detected SLF spectra of Vpu TM at 25 °C are shown in Figure 5. The spectra were recorded using $R18^{7}_{1}$ pulses for hetero-nuclear dipolar recoupling under 11 kHz MAS. ^{1}H-^{15}N dipolar coupling and ^{1}H-^{13}C dipolar coupling frequencies were encoded in a constant time spin echo period with refocusing of chemical shifts. Dipolar frequencies were measured for evolution periods of 4.68 ms for ^{1}H-^{15}N DC and 2.88 ms for ^{1}H-^{13}C DC. For ^{1}H-$^{15}N/^{13}C\alpha$ correlations, DCP was used to transfer coherence from ^{15}N to $^{13}C\alpha$ sites using the pulse sequence shown in Figure 1A without the inclusion of ^{15}N shift evolution and spin diffusion periods. In a similar fashion, ^{1}H-^{13}C dipolar coupling frequencies were measured using the pulse sequence shown in Figure 1C without incorporation of spin-diffusion period and direct detection of ^{13}C shifts. As can be seen from the figure several distinguishable cross-peaks are observed for a single chemical shift. This is mainly due to the magnetic in-equivalence in the helix caused by the topological arrangement relative to the bilayer normal. For example, in Figure 5A, a single chemical shift at 53.5 ppm has at least three resolved cross peaks in the ^{1}H-^{15}N dipolar frequency dimension. Similar resolution is also observed for ^{1}H-^{13}C dipolar coupling frequencies (Figure 4B). Even though the introduction of the dipolar coupling frequencies is a step forward in resolution enhancement for residues with very similar or identical chemical shifts, complete resolution is not achievable for Val and Ile residues using two-dimensional experiments.

Resolution in three-dimensional spectra

Superior resolution is observed in three-dimensional separated local field experiments with the incorporation of ^{15}N chemical shift frequencies. Three-dimensional SLF spectra correlating ^{1}Hα-^{13}Cα and ^{1}H-^{15}N DCs with ^{15}N and ^{13}Cα shifts were acquired using the pulse schemes diagrammed in Figure 1A and D. The spectra were recorded with 2.16 ms ^{1}H-^{13}C and 3.76 ms ^{1}H-^{15}N dipolar evolution, and 6 ms ^{15}N and 10 ms ^{13}C evolution for indirect and direct detection. Two-dimensional SLF planes correlating ^{1}H-^{15}N/^{13}Cα and ^{1}Hα-^{13}Cα/^{13}Cα at ^{15}N shift frequencies are shown in Figure 6A–D. Figure 6A and C represent the ^{1}H-^{15}N/^{13}Cα and ^{1}Hα-^{13}Cα/^{13}Cα planes at the 121.6 ppm ^{15}N chemical shift frequency. Three distinguishable ^{1}H-^{13}C dipolar frequencies are observable compared to a single ^{1}H-^{15}N dipolar frequency at a single resonance for valine. The two-dimensional SLF planes shown in Figure 6B and D were extracted at the 122.8 ppm ^{15}N chemical shift frequency. Isotropic shifts attributed to Ala residues show three well-resolved contours for ^{1}H-^{15}N dipolar frequencies compared to two signals with ^{1}H-^{13}C dipolar frequencies. Somewhat better resolution was achieved in a three-dimensional experiment correlating ^{1}H-^{15}N and ^{1}Hα-^{13}Cα dipolar frequencies with ^{13}Cα isotropic shifts using the pulse sequence shown in Figure 1D. The two-dimensional SLF planes correlating ^{1}H-^{15}N DCs with ^{1}Hα-^{13}Cα DCs extracted at 65.7 ppm and 53.5 ppm ^{13}Cα shifts are shown in Figure 6E and F. The dipolar frequencies were encoded in constant spin echo periods for 5.12 ms ^{1}H-^{15}N and 2.88 ms ^{1}H-^{13}C dipolar evolutions, respectively.

The three-dimensional spectrum correlating ^{1}H-^{13}C DCs with ^{13}C/^{13}C shifts was acquired using the pulse scheme shown in Figure 1C. The spectrum was recorded with a 2.16 ms dipolar evolution, and 5 ms/10 ms ^{13}C evolution for indirect/direct detection. Homonuclear correlation was established using 50 ms PDSD mixing and 100 μs cross-polarization mixing during preparation. The two-dimensional ^{13}C/^{13}C correlation plane correlated to 9.9 kHz ^{1}H-^{13}C DC is shown in Figure 6G. Each cross peak in the two-dimensional planes corresponds to a single site resolution.

Dipolar Assisted Assignment Protocol (DAAP)

Irrespective of single site resolution in three-dimensional SLF experiments, measurement of dipolar frequencies is still ambiguous due to the degeneracy in ^{15}N and ^{13}Cα chemical shits. Here we illustrate how the new assignment protocol assists in the assignment of chemical shift and dipolar frequencies. The three-dimensional experiments correlating dipolar coupling and chemical shift frequencies are used for establishing sequential assignments in backbone and side chain atoms similar to chemical shift assignment experiments such as NCACO, NCOCA and CANCO. A three-dimensional correlation ^{1}H-^{15}N DC/^{15}N CS/^{13}CX CS spectrum is shown in Figure 7. The experiments correlating ^{1}H-^{15}N DC with N(CA)CX or N(CO)CX heteronuclear correlation were obtained using the pulse sequence diagrammed in Figure 1A. Cross-polarization from ^{15}N to either ^{13}Cα or ^{13}CO was performed using 3 ms DCP mixing. Homo-nuclear polarization transfer was carried out with 20 ms DAAR. A two-dimensional plane correlating ^{15}N/^{13}C chemical shifts obtained at a ^{1}H-^{15}N dipolar coupling frequency of 2.4 kHz is shown in Figure 7A. The intra-residue correlation spectrum was assigned to Val residue (V13) in the sequence. Similarly, a two-dimensional plane correlating ^{13}CO and ^{13}Cα chemical shifts of V13 to the ^{15}N chemical shift of A14 was

obtained for ^{1}H-^{15}N dipolar coupling frequency at 2.55 kHz. Both intra- and inter- residue shift correlation with ^{1}H-^{15}N dipolar frequencies was obtained using the pulse sequence shown in Figure 1B. In this experiment, the ^{13}CO chemical shift of the preceding residue (i-1) is correlated with ^{1}H-^{15}N dipolar coupling and the ^{15}N, $^{13}C\alpha$ chemical shift frequencies of the same residue (i). Figure 7C represents the two-dimensional plane correlating the ^{13}CO chemical shift of V13 to the ^{15}N and $^{13}C\alpha$ chemical shifts of A14. The two-dimensional plane was obtained for 2.55 kHz ^{1}H-^{15}N dipolar frequency. Following the chemical shifts and dipolar correlation, ^{1}H-^{15}N dipolar frequencies at 2.4 kHz and 2.55 kHz were assigned to V13 and A14 respectively.

Three-dimensional data correlating ^{1}H-^{13}C DC/^{13}C CS/^{13}C CS frequencies were obtained using the pulse scheme shown in Figure 1C. A two-dimensional plane with ^{13}C/^{13}C shift correlation at a dipolar coupling frequency of 7.4 kHz is shown in Figure 6D. The correlation of $^{13}C\alpha$ with ^{13}CO and side chain carbons is observed at a selected $^{1}H\alpha$-$^{13}C\alpha$ dipolar frequency. The other advantage of this experiment is that side chain dipolar frequencies are also observable, opening up a promising path to resolution, assignment, and structure determination of the side chains. Thus, DAAP is applicable to both backbone and side chain sites. However, data for side chains are not included here because this topic is well beyond the scope of the current discussion. Following the method of dipolar coupling and chemical shift correlation spectroscopy supplemented by the dipolar assisted assignment protocol, the dipolar frequencies and chemical shifts of all residues in Vpu TM were assigned unambiguously. These are collated in Table 1 and Figure 8.

Rotationally aligned solid-state NMR and structure determination of a transmembrane helix

^{1}H–^{15}N dipolar coupling values measured for each residue in Vpu TM are plotted as a function of the residue number in Figure 8A. A characteristic Dipolar Wave pattern is observed that enables helical segments of the protein to be readily identified and characterized with respect to the helix length, helix orientation in the membrane, and presence of any kinks [38]. Notably, the ^{1}H–^{15}N DC values measured here for Vpu TM in proteoliposomes (open circles) are very similar to the values measured previously for the same protein in mechanically aligned bilayers (cross marks) and magnetically aligned bilayers (q = 3.2 bicelles), demonstrating that information obtained from motion averaged powder patterns of proteins in liposomes, recoupled under MAS, is the same as that from single line OS solid-state NMR spectra of uniaxially aligned proteins.

The experimental measurements from an aligned, stationary bicelle sample were taken from an earlier publication. Although there is some variation in the ^{1}H-^{15}N dipolar coupling values that are plotted, most points are nearly identical, and they all fall within the 10% estimated margin of error and reproducibility. The original measurements of 1H-15N dipolar coupling in DMPC bilayers on glass plates yielded a value of 27°, and in DMPC bicelles a value of 30°. Here the calculation in DMPC proteoliposomes include both 1H-15N and 1H-13C dipolar couplings, and yield a value of 28°. Taking into account the somewhat different sample conditions and different experimental methods, we consider all of these values to be consistent [39] [22].

Summary

The ambiguities in resonance assignments of membrane proteins are mainly due to the poor chemical shift dispersion. However, rotational alignment resulting from the global motion of the protein provides variation in the dipolar frequency for residues those are chemically equivalent but magnetically inequivalent. Here, we show experimental methods that correlate dipolar coupling frequencies with isotropic chemical shifts to enhance spectral resolution and aid in making resonance assignments. We refer to this as a dipolar assisted assignment protocol. In DAAP, ^{13}C chemical shift resonance frequencies, mainly ^{13}Cα and ^{13}CO, within a residue are correlated to the ^{15}N chemical shift resonances and ^{1}H-^{15}N dipolar coupling frequencies of adjacent residues. The correlations were established using the three-dimensional experiments diagrammed in Figure 1. In these experiments, the ^{1}H-^{15}N dipolar coupling frequencies are correlated to the resonances observed in two-dimensional heteronuclear N(CA)CX, N(CO)CX and CANCO correlation spectra. The results are shown in Figures 3 – 7 for a uniform ^{13}C, ^{15}N labeled membrane protein. Single site resolution for nearly all resonances is observed. Variation in dipolar frequencies adds further resolution to the severely crowded spectra obtained from chemical shift correlation alone. Unambiguous assignment of residues is made possible due to the gain in resolution. These pulse schemes can also be used for isotope labeled and partial isotope labeled samples. As shown in the results, the method also benefits with accurate measurement of dipolar frequencies for residues with similar ^{13}C and ^{15}N chemical shifts. It is now possible to assign and measure dipolar frequencies in a sequential manner. Dipolar waves are compared for results obtained from two sample preparation methods for Vpu TM in phospholipid bilayers. Very similar dipolar waves confirm the similar topological arrangement for the protein whether made from uniaxially oriented samples from mechanical alignment in phospholipid bilayers or magnetically aligned bicelles or rotationally aligned unoriented proteoliposome. Equivalent angular constraints are measured from the unoriented proteoliposome samples using the pulse sequences reported in this article. The pulse schemes can also be extended to higher dimensions to obtain superior resolution. For instance, Figure 1A can readily be extended to a four-dimensions by adding ^{13}Cα or ^{13}CO chemical shift evolutions after DCP transfer. In a similar fashion Figure 1B can be extended to a pseudo 4D or 5D experiments to measure ^{13}C-^{15}N dipolar couplings. This can be achieved by adding a variable mixing period for TEDOR transfer and incorporating ^{13}C shift evolution after CP. In the future, it should also be possible to perform ^{1}H NMR analogs of these experiments [40]. These methods can be readily extended to side chain resonances, enabling complete structure determinations of membrane proteins.

References

1. McDermott A. Structure and dynamics of membrane proteins by magic angle spinning solid-state NMR. Annu Rev Biophys. 2009; 38:385–403. [PubMed: 19245337]
2. Opella SJ. Structure Determination of Membrane Proteins by Nuclear Magnetic Resonance Spectroscopy. Annual Review of Analytical Chemistry. 2013; 6:305–328.
3. Schuetz A, Wasmer C, Habenstein B, Verel R, Greenwald J, Riek R, Böckmann A, Meier BH. Protocols for the Sequential Solid-State NMR Spectroscopic Assignment of a Uniformly Labeled 25 kDa Protein: HET-s(1–227). ChemBioChem. 2010; 11:1543–1551. [PubMed: 20572250]

4. Shi L, Lake EM, Ahmed MA, Brown LS, Ladizhansky V. Solid-state NMR study of proteorhodopsin in the lipid environment: secondary structure and dynamics. Biochimica et Biophysica Acta (BBA)-Biomembranes. 2009; 1788:2563–2574.
5. Tang W, Knox RW, Nevzorov AA. A spectroscopic assignment technique for membrane proteins reconstituted in magnetically aligned bicelles. J Biomol NMR. 2012; 54:307–316. [PubMed: 22976525]
6. Ikeda K, Egawa A, Fujiwara T. Secondary structural analysis of proteins based on (13)C chemical shift assignments in unresolved solid-state NMR spectra enhanced by fragmented structure database. J Biomol NMR. 2013; 55:189–200. [PubMed: 23271376]
7. Das BB, Nothnagel HJ, Lu GJ, Son WS, Tian Y, Marassi FM, Opella SJ. Structure determination of a membrane protein in proteoliposomes. J Am Chem Soc. 2012; 134:2047–2056. [PubMed: 22217388]
8. Hefke F, Bagaria A, Reckel S, Ulrich SJ, Dotsch V, Glaubitz C, Guntert P. Optimization of amino acid type-specific 13C and 15N labeling fo the backbone assignment of membrane proteins by solution- and solid-state NMR with the UPLABEL algorithm. J Biomol NMR. 2011; 49:75–84. [PubMed: 21170670]
9. Cone RA. Rotational Diffusion of Rhodopsin in the Visual Receptor membrane. Nature New Biology. 1972; 236:39–43.
10. Edidin M. Rotational and Translational Diffusion in Membranes. Annual Review of Biophysics and Bioengineering. 1974; 3:179–201.
11. McConnell HM, Hubbell WL. Molecular motion in spin-labeled phospholipids and membranes. J Am Chem Soc. 1971; 93:314–326. [PubMed: 5541516]
12. Poo MM, Cone RA. Lateral diffusion of rhodopsin in the photoreceptor membrane. Nature. 1974; 247:438–441. [PubMed: 4818543]
13. Cherry RJ. Protein mobility in membranes. FEBS Letters. 1975; 55:1–7. [PubMed: 237788]
14. CRR, McLaughlin AC, Hemming MA, Hoult DI, Radda GK, Ritchie GA, Seeley PJ, Richards RE. Application of 31P NMR to model and biological membrane systems. FEBS Lett. 1975; 57:1–7. [PubMed: 1175769]
15. Park SH, Mrse AA, Nevzorov AA, De Angelis AA, Opella SJ. Rotational diffusion of membrane proteins in aligned phospholipid bilayers by solid-state NMR spectroscopy. J Magn Reson. 2006; 178:162–165. [PubMed: 16213759]
16. Lewis B, Harbison G, Herzfeld J, Griffin RG. NMR structural analysis of a membrane protein: bacteriorhodopsin peptide backbone orientation and motion. Biochemistry. 1985; 24:4671–4679. [PubMed: 4063350]
17. Marassi FM, Das BB, Lu GJ, Nothnagel HJ, Park SH, Son WS, Tian Y, Opella SJ. Structure determination of membrane proteins in five easy pieces. Methods. 2011; 55:363–369. [PubMed: 21964394]
18. Park SH, Casagrande F, Das BB, Albrecht L, Chu M, Opella SJ. Local and global dynamics of the G protein-coupled receptor CXCR1. Biochemistry. 2011; 50:2371–2380. [PubMed: 21323370]
19. Park SH, Das BB, De Angelis AA, Scrima M, Opella SJ. Mechanically, Magnetically, and "Rotationally Aligned" Membrane Proteins in Phospholipid Bilayers Give Equivalent Angular Constraints for NMR Structure Determination. The Journal of Physical Chemistry B. 2010; 114:13995–14003. [PubMed: 20961141]
20. Gutowsky HS, Pake GE. Structural investigations by means of nuclear magnetism. II. Hindered rotation in solids. J Chem Phys. 1950; 18:162–170.
21. Mehring M, Griffin RG, Waugh JS. 19F Shielding tensors from coherently narrowed NMR powder spectra. J Chem Phys. 1971; 55:746–755.
22. Park SH, De Angelis AA, Nevzorov AA, Wu CH, Opella SJ. Three-dimensional structure of the transmembrane domain of Vpu from HIV-1 in aligned phospholipid bicelles. Biophys J. 2006; 91:3032–3042. [PubMed: 16861273]
23. Thaukur RS, Kurur ND, Madhu PK. Swept-frequency two-pulse phase odulation for heteronuclear dipolar decoupling in solid-state NMR. Chem Phys Lett. 2006; 426:459–463.
24. Shaka AJ, Keeler JM, Freeman R. Evaluation of a new broadband decoupling sequence: WALTZ-16. J Magn Reson. 1983; 53:313–340.

25. Pines A, Gibby MG, Waugh JS. Proton-enhanced NMR of dilute spins in solids. J Chem Phys. 1973; 59:569–590.
26. Baldus M, Petkova AT, Herzfeld J, Griffin RG. Cross polarization in the tilted frame: assignment and spectral simplification in heteronuclear spin systems. Molecular Physics. 1998; 95:1197–1207.
27. Jaroniec CP, Filip C, Griffin RG. 3D TEDOR NMR Experiments for the Simultaneous Measurement of Multiple Carbon-Nitrogen Distances in Uniformly 13C, 15N-Labeled Solids. J Am Chem Soc. 2002; 124:10728–10742. [PubMed: 12207528]
28. Szeverenyi NM, Sullivan MJ, Maciel GE. Observation of spin exchange by two-dimensional fourier transform 13C cross polarization-magic-angle spinning. Journal of Magnetic Resonance (1969). 1982; 47:462–475.
29. Suter D, Ernst R. Spin diffusion in resolved solid-state NMR spectra. Physical Review B. 1985; 32:5608–5627.
30. Grommek A, Meier BH, Ernst M. Distance information from proton-driven spin diffusion under MAS. Chemical physics letters. 2006; 427:404–409.
31. Dumez JN, Halse ME, Butler MC, Emsley L. A first-principles description of proton-driven spin diffusion. Phys Chem Chem Phys. 2011; 14:86–89. [PubMed: 22086134]
32. Takegoshi K, Nakamura S, Terao T. 13C-1H dipolar-assisted rotational resonance in magic-angle spinning NMR. Chemical Physics Letters. 2001; 344:631–637.
33. Zhao X, Eden M, Levitt MH. Recoupling of heteronuclear dipolar interactions in solid-state NMR using symmetry-based pulse sequences. Chemical Physics Letters. 2001; 342:353–361.
34. Waugh JS. Uncoupling of local field spectra in nuclear magnetic resonance: Determination of atomic position in solids. Proc Natl Acad Sci U S A. 1976; 73:1394–1397. [PubMed: 1064013]
35. Herzfeld J, Berger AE. Sideband intensities in NMR spectra of samples spinning at the magic angle. The Journal of Chemical Physics. 1980; 73:6021–6030.
36. Loening NM, Bierring M, Nielsen NC, Oschkinat H. A comparison of NCO and NCS transfer methods for biological solid-state NMR spectroscopy. J Magn Reson. 2012; 214:81–90. [PubMed: 22116035]
37. Zhao X, Hoffbauer W, Schmedt auf der Günne J, Levitt MH. Heteronuclear polarization transfer by symmetry-based recoupling sequences in solid-state NMR. Solid state nuclear magnetic resonance. 2004; 26:57–64. [PubMed: 15276635]
38. Mesleh MF, Veglia G, DeSilva TM, Marassi FM, Opella SJ. Dipolar waves as NMR maps of protein structure. J Am Chem Soc. 2002; 124:4206–4207. [PubMed: 11960438]
39. Park SH, Opella SJ. Tilt angle of a trans-membrane helix is determined by hydrophobic mismatch. Journal of molecular biology. 2005; 350:310–318. [PubMed: 15936031]
40. Hou G, Paramasivam S, Yan S, Polenova T, Vega AJ. Multidimensional magic angle spinning NMR spectroscopy for site-resolved measurement of proton chemical shift aniotropy in biological solids. J Am Chem Soc. 2013; 135:1358–1368. [PubMed: 23286322]

Highlights

- Equivalent angular constraints are obtained for MAS of rotationally aligned Vpu TM in phospholipid bilayers.
- Pulse sequences for dipolar assisted assignment protocol are presented.
- Multi-dimensional experiments are proposed to measure chemical shifts and dipolar frequencies in rotationally aligned membrane proteins.
- Chemical shift and dipolar frequency correlation provide high resolution and assist in unambiguous resonance assignment.

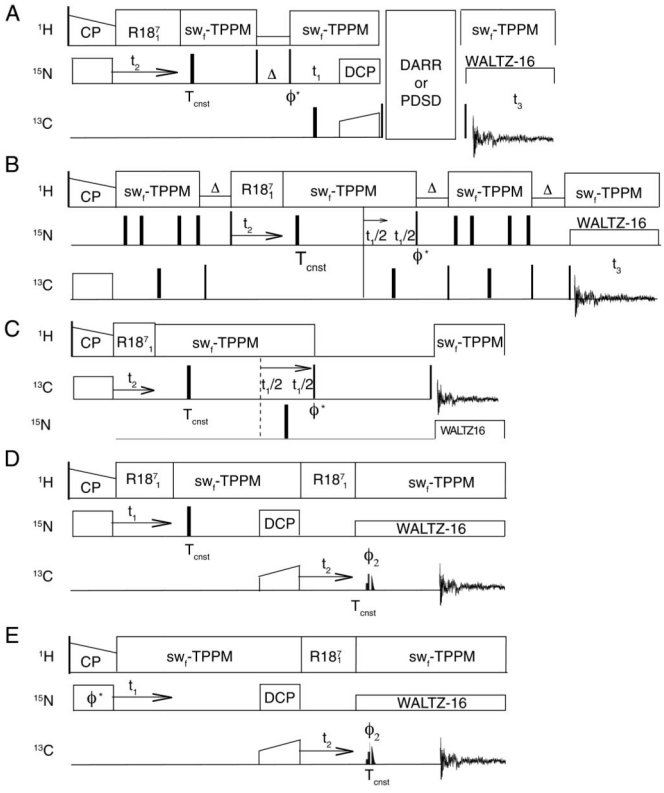

Figure 1.

Multidimensional pulse schemes for dipolar assisted assignment protocol experiments. (A) Intra or inter residue correlation of ^{1}H-^{15}N DC/^{15}N(Cα)^{13}CX or ^{1}H-^{15}N DC/^{15}N(C)^{13}CX. (B) ^{1}H-^{15}N DC/^{13}Cα^{15}N^{13}CO. (C) ^{1}Hα-^{13}Cα DC/^{13}C CS/^{13}C CS. (D) ^{1}H-^{15}N DC/^{1}Hα-^{13}Cα DC/^{13}Cα CS. (E) ^{1}Hα-^{13}Cα DC/^{15}N CS/^{13}Cα CS. Thin and wide solid lines are for 90° and 180° pulses. Delta symbol represents the delay for z-filter. CP and DCP represents cross polarization and double cross polarization under SPECIFIC CP condition. CS stands for chemical shift φ represents the phase change under States mode.

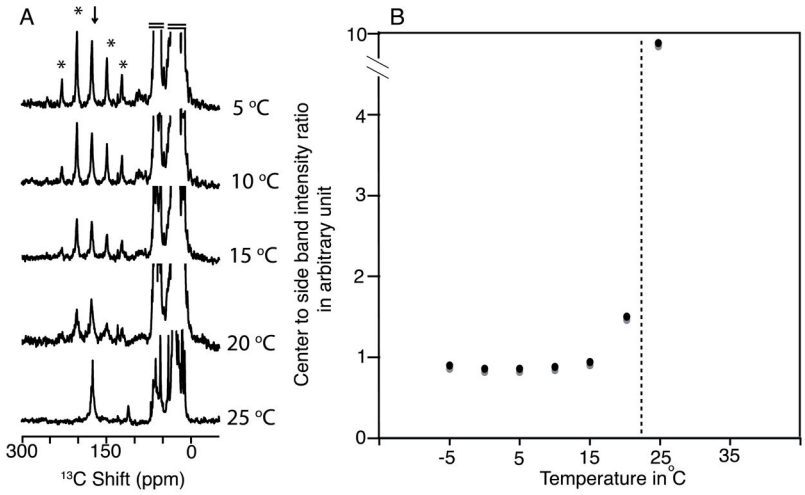

Figure 2.

Rotational alignment of uniformly ^{13}C,^{15}N labeled single trans-membrane helix from Vpu in DMPC proteoliposome. (A) ^{13}C detected one-dimensional spectra recorded at various temperatures ranging from 5 °C to 25 °C. Data were collected using ^{1}H to ^{13}C cross-polarization under 5 kHz magic angle sample spinning. (B) Graphical plot showing the variation in intensity ratios (central peak to the first sideband on the left) as a function of temperature. Central peak is marked with an arrow in A and asterisks denote spinning side bands. One-dimensional data were acquired with 100 kHz spectral width, 15 ms acquisition time, and 2 s recycle delay for 16 scans (5 °C), 32 scans (10 °C, 15 °C, 20 °C) and 64 scans (25 °C).

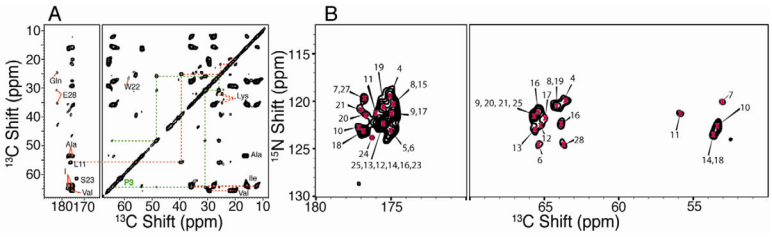

Figure 3.

^{13}C detected two-dimensional correlation spectra of uniformly ^{13}C, ^{15}N labeled Vpu-TM. (A) ^{13}C/^{13}C correlation spectrum obtained from 50 ms proton driven spin diffusion (PDSD) mixing. Single resonance assignment for ^{13}C shifts in P3, L11and S23 are labeled. Chemical shift dispersion for other residues such as Ala, Val, Ile, Glu, Gln, Trp, and Lys are also been labeled. (B) Two-dimensional N(CA)CX correlation spectra. 20 ms DARR mixing was used for carbon spin exchange in B. Residue numbers are marked following the sequential resonance assignment. Homo- and hetero- nuclear correlation two-dimensional spectra were acquired with 128 scans (^{13}C/^{13}C) and 512 scans (^{13}C/^{15}N) with a 2 s recycle delay. Experiments were carried out with 242 ppm (^{13}C), 80 ppm (^{13}C) and 32 ppm (^{15}N) spectral widths for direct and indirect acquisition. The acquisition periods were 12 ms for direct and 4 ms (^{13}C)/6 ms (^{15}N) for indirect detection. 100 μs, 500 μs and 3000 μs contact times were used for ^{1}H to ^{13}C, ^{1}H to ^{15}N and ^{15}N to ^{13}C cross-polarization, respectively.

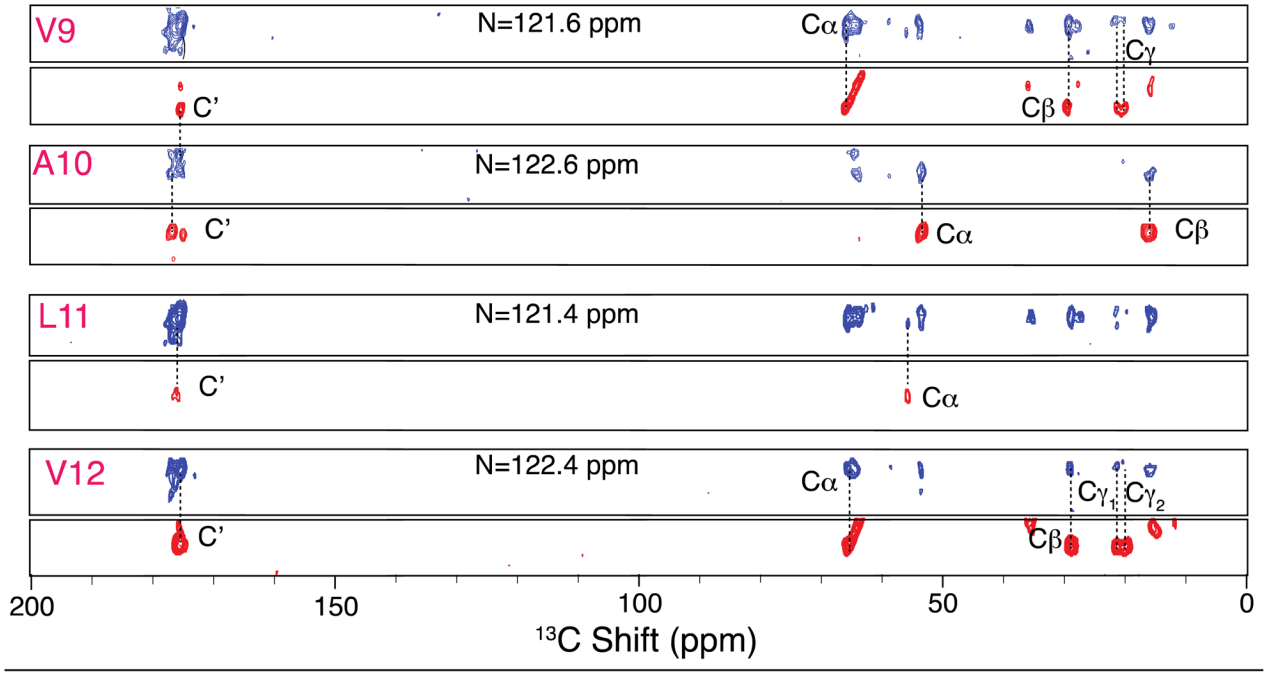

Figure 4.

Strip-plots for resonance assignment for residues V9–V12 in uniformly ^{13}C,^{15}N labeled Vpu TM. Two-dimensional $^{13}C/^{13}C$ correlation plot from NCACX (red) and NCOCX (blue) data extracted at ^{15}N shifts. ^{13}C shifts are marked according to their positions in backbone and side chains. Three-dimensional data were acquired with 256 scans (NCACX) and 512 scans (NCOCX). The experiments were carried out under similar conditions to those described in Figure 3 except that the homonuclear spin diffusion was obtained with 40 ms DARR mixing, and 40 ppm and 20 ppm ^{13}C spectral widths for NCACX and NCOCX, respectively.

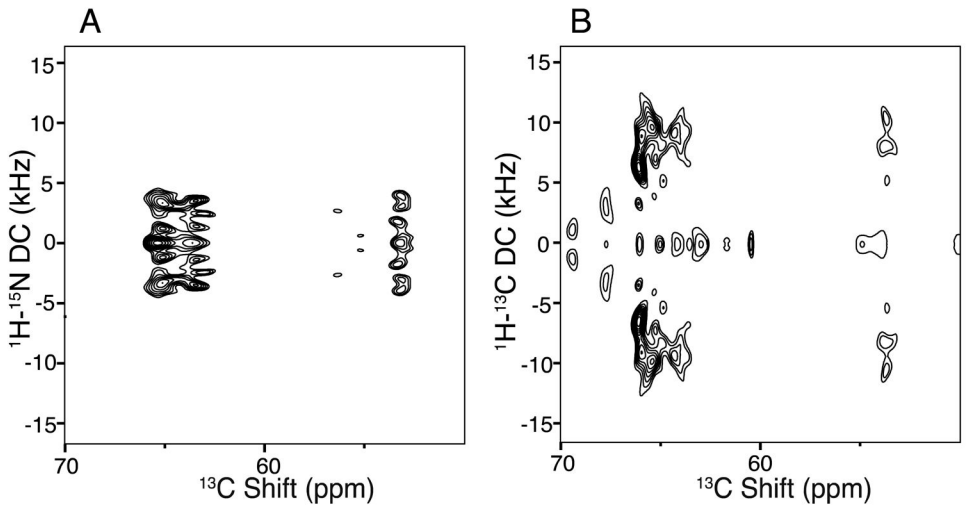

Figure 5.

^{13}C-detected two-dimensional separated local field NMR spectra. (A) ^{15}N edited spectrum correlating ^{13}Cα chemical shifts and ^{1}H-^{15}N dipolar couplings. The spectrum was obtained using the pulse scheme shown in Figure 1A without the ^{15}N chemical shift evolution and spin diffusion mixing periods. (B) ^{13}C CS/^{1}H-^{13}C DC correlation spectrum. All spectra were recorded under 11.111 kHz MAS at 25 °C. Two-dimensional data were acquired with 512 scans (A) and 128 scans (B) using a 2 s recycle delay. Dwell times of 90 μs for A and 30 μs for B were used in the indirect dimensions to record the spectra. A 12 ms acquisition time was used for direct ^{13}C detection.

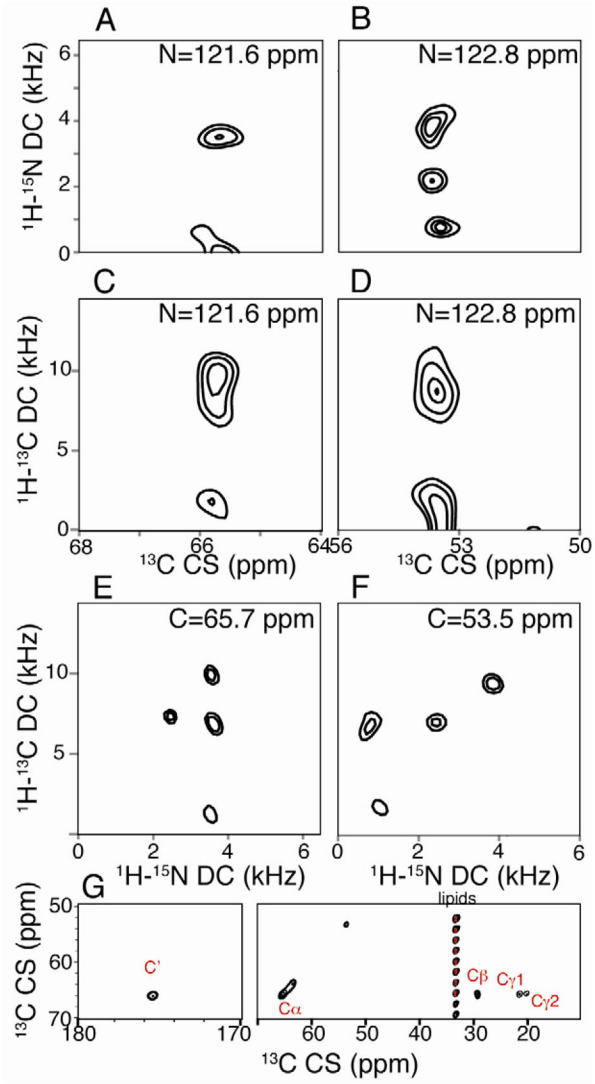

Figure 6.

^{13}C detected three-dimensional separated local field spectra of uniformly ^{13}C,^{15}N labeled Vpu TM. (A) and (B) Two-dimensional SLF planes correlating ^{13}Cα CS/^{1}H-^{15}N DC extracted from a three-dimensional SLF data set for ^{15}N shifts at 121.6 ppm and 122.8 ppm, respectively. The spectrum was recorded using the pulse scheme shown in Figure 1A without incorporating the spin diffusion mixing. (C) and (D) Two-dimensional SLF planes correlating ^{13}Cα CS/^{1}Hα-^{13}Cα DC for ^{15}N shifts at 121.6 ppm and 122.8 ppm, respectively. The experiment correlating ^{13}Cα CS/^{15}N CS/^{1}Hα-^{13}Cα DC was acquired using the pulse scheme in Figure 1E. (E) and (F) Two-dimensional SLF planes correlating ^{1}H-^{15}N/^{1}Hα-^{13}Cα dipolar frequencies extracted from a three-dimensional SLF data set for ^{13}C shifts at 65.7 ppm and 53.5 ppm, respectively. The three-dimensional data was collected using the pulse scheme in Figure 1D. (G) ^{13}C/^{13}C two-dimensional plane obtained at 9.9 kHz ^{1}Hα-^{13}Cα DC. Three-dimensional SLF data correlating ^{1}Hα-^{13}Cα DC/^{13}C CS/^{13}C CS recorded using the pulse scheme shown in Figure 1C. All spectra were collected at a spinning frequency of 11.111 kHz and 25 °C sample temperature. t1 noise

from lipid signals is denoted with asterisks. The three-dimensional data in A–F were collected with 512 scans (A–F) or128 scans (G). A 2 s recycle delay and 90 μs dwell time were used in the experiments.

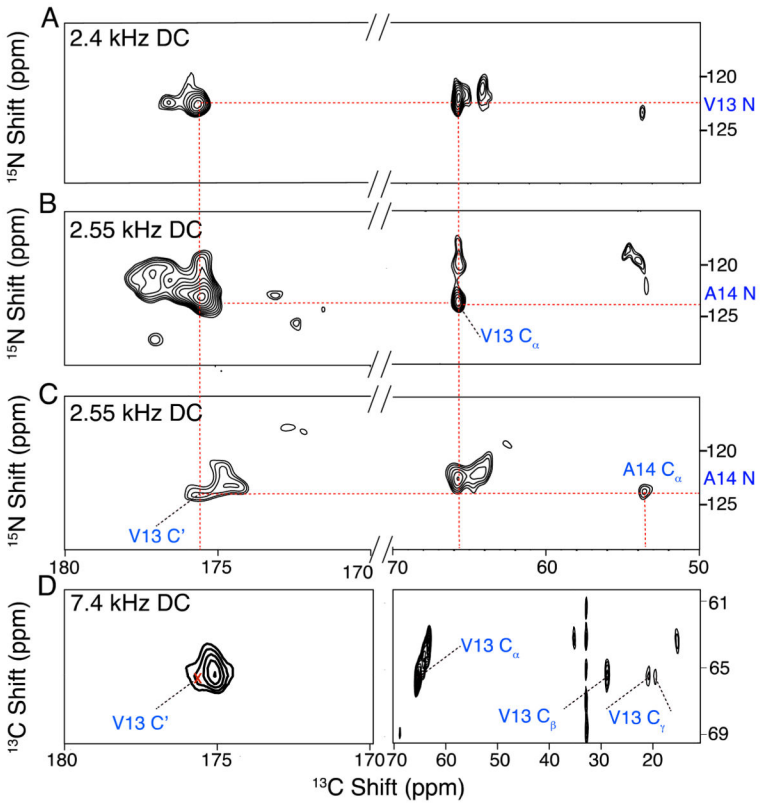

Figure 7.

^{13}C detected three-dimensional SLF data correlating ^{13}C and ^{15}N isotropic chemical shifts with ^{1}H-^{15}N dipolar frequencies. (A) N(CA)CX two-dimensional plane obtained at 2.4 kHz ^{1}H-^{15}N dipolar coupling (DC) frequency. The three-dimensional data were collected using the pulse scheme shown in Figure 1A with a 20 ms DARR (dipolar assisted rotational resonance) mixing. (B) N(CO)CX 2D-plane at 2.55 kHz ^{1}H-^{15}N DC. The three-dimensional data were collected using the pulse scheme shown in Figure 1A with 40 ms DARR mixing. (C) CONCA two-dimensional correlation plane obtained for 2.55 kHz ^{1}H-^{15}N DC. The three-dimensional data were collected using the pulse scheme shown in Figure 1B with 1.44 ms TEDOR mixing. Dashed lines illustrate the connectivity for residues A14 and V13 for ^{15}N and ^{13}C shifts. (D) ^{13}C/^{13}C two-dimensional plane obtained at 7.4 kHz ^{1}Hα-^{13}Cα DC. Three-dimensional SLF data correlating ^{1}Hα-^{13}Cα DC/^{13}C CS/^{13}C CS recorded using the pulse scheme shown in Figure 1C. The three-dimensional data were collected with 1024 scans (A–C), 128 scans (D), 2 s recycle delay and 90 μs dwell time.

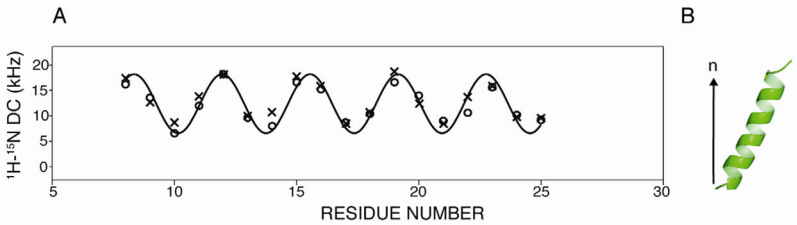

Figure 8.

Dipolar wave plot for ^{1}H-^{15}N dipolar frequencies as a function of residue type. Comparison between the dipolar waves of normalized dipolar couplings (x) with order parameter S = 0.8 obtained from 14-O-PC/6-O-PC bicelles (q = 3.2) at 42°C and those of dipolar couplings (o) obtained from DMPC liposomes at a spinning rate of 11.111 kHz and 25°C.

Table 1

Residue	^{15}N shift (ppm)	^{13}CA shift (ppm)	^{13}CO shift (ppm)	^{15}N-^{1}H coupling (kHz)	^{13}Cα-^{1}Hα coupling (kHz)
I6	124.3	64.9	175.6	2.4	20.7
A7	120.3	53.7	177.0	3.6	14.0
I8	120.6	63.9	175.2	16.2	21.5
V9	121.6	65.9	175.2	13.6	19.6
A10	122.6	53.7	176.8	6.6	
L11	121.4	56.0	176.0	12.0	4.4
V12	122.2	65.7	175.1	18.2	21.0
V13	123.0	66.0	175.3	9.6	7.4
A14	122.5	53.8	175.0	8.0	20.0
I15	120.8	64.0	175.1	16.6	16.3
I16	122.6	64.5	175.5	15.2	19.1
I17	121.3	64.9	175.3	8.7	8.6
A18	122.6	53.8	176.8	10.4	14.5
I19	121.1	64.3	175.3	16.6	2.2
V20	121.8	65.9	176.1	14.0	14.0
V21	121.0	65.8	175.8	9.0	15.0
W22	122.7	58.0	178.1	10.6	2.4
S23		61.7	175.3	15.6	19.3
I24	124.2	64.4	176.2	10.2	19.0
V25	121.7	65.9	175.7	9.2	18.1